Published in final edited form as:
Science. 2013 January 25; 339(6118): . doi:10.1126/science.1232251.

Actin, spectrin and associated proteins form a periodic cytoskeletal structure in axons

Ke Xu[1,†], **Guisheng Zhong**[1,†], and **Xiaowei Zhuang**[1,2,*]

[1]Howard Hughes Medical Institute, Department of Chemistry and Chemical Biology, Harvard University, Cambridge, MA 02138, USA

[2]Department of Physics, Harvard University, Cambridge, MA 02138, USA

Abstract

Actin and spectrin play important roles in neurons, but their organization in axons and dendrites remains unclear. We used stochastic optical reconstruction microscopy (STORM) to study the organization of actin, spectrin and associated proteins in neurons. Actin formed ring-like structures that wrapped around the circumference of axons and evenly spaced along axonal shafts with a periodicity of ~180–190 nm. This periodic structure was not observed in dendrites, which instead contained long actin filaments running along dendritic shafts. Adducin, an actin-capping protein, colocalized with the actin rings. Spectrin exhibited periodic structures alternating with those of actin and adducin, and the distance between adjacent actin-adducin rings was comparable to the length of a spectrin tetramer. Sodium channels in axons were distributed in a periodic pattern coordinated with the underlying actin-spectrin-based cytoskeleton.

Actin plays critical roles in shaping and maintaining cell morphology, as well as in supporting cellular various functions, including cell motility, cell division, and intracellular transport (1). In neurons, actin is essential for the establishment of neuronal polarity, the transport of cargos, the growth of neurites, and the stabilization of synaptic structures (2–4). Despite its importance, our understanding of actin structures in neurons remains incomplete. Electron microscopy has provided detailed actin ultrastructure in growth cones and dendritic spines (5, 6), where actin is the dominant cytoskeletal protein, but little is known about the organization of actin in the axonal and dendritic shafts (4). Though neurites often have sub-micrometer diameters, they contain a high density of different types of cytoskeletal filaments, such as microtubules and neurofilaments (6–8). Hence, resolving the organization of actin in axons and dendrites is challenging, requiring imaging tools with both high spatial resolution and molecular specificity.

A prototypical actin-spectrin-based cytoskeleton structure is found in red blood cells (erythrocytes) (9, 10), where actin, spectrin and associated proteins form a two-dimensional (2D) polygonal network (mostly comprised of hexagons and pentagons) underneath the erythrocyte membrane (11, 12). Spectrin analogues have been found in many other animal cells (9, 10), including neurons (13, 14). They play important roles, ranging from the regulation of the heartbeat, to the stabilization of axons, the formation of axon initial segments and nodes of Ranvier, and the stabilization of synapses in neurons (9, 10, 15). An

*To whom correspondence should be addressed. zhuang@chemistry.harvard.edu.
†These authors contributed equally to this work.

Supplementary Materials
Materials and Methods
References 38–42
Figs. S1 to S10

erythrocyte-like, polygonal lattice structure has been observed for spectrin in the drosophila neuromuscular junction (16), and models similar to the erythrocyte cytoskeleton have also been proposed for other systems (10). However, the ultrastructural organization of spectrin in non-erythrocyte cells is largely unknown due to similar challenges in imaging.

Recent advances in super-resolution fluorescence microscopy (17, 18) allow resolutions down to ~10 nm to be achieved with molecular specificity, providing a promising solution to the above challenges. In particular, super-resolution studies of neurons have provided valuable structural and dynamic information of actin in dendritic spines (19–22). In this work, we studied the three-dimensional (3D) ultrastructural organization of actin and spectrin in neurons using a super-resolution fluorescence imaging method, stochastic optical reconstruction microscopy (STORM) (23–27).

To image actin in neurons, we fixed cultured rat hippocampal neurons at various days in vitro (DIV), and labeled actin filaments with phalloidin conjugated to a photoswitchable dye, Alexa Fluor 647 (Fig. 1) (28). To identify axons and dendrites, we immunolabeled MAP2, a microtubule associate protein enriched in dendrites, or NrCAM, a cell adhesion molecule found in the initial segments of axons (15), using a dye of a different color (Fig. 1) (28). In the conventional fluorescence images (Fig. 1A, D, F), MAP2 specifically stained dendrites and NrCAM specifically labeled the initial segments of axons, whereas actin was found in both dendrites and axons.

Next, we imaged the ultrastructure of actin using 3D STORM (27) with a dual-objective astigmatism-imaging scheme (28, 29). Only a sparse subset of the labeled Alexa 647 molecules were activated with 405 nm light at any instant and imaged with 647 nm light using a continuous illumination and detection mode (30). The x-y and z coordinates of the activated molecules were determined from the centroid positions and ellipticity values of their images, respectively (27, 29). Iterating this procedure allowed numerous molecules to be localized and a 3D super-resolution image to be constructed from the coordinates of these molecules.

In contrast to the conventional images, individual actin filaments were resolved in the STORM images (Fig. 1B, C, E, G and Fig. S1B) (28). Long actin filaments were observed in dendrites (Fig. 1B, C and Fig. S1B). These filaments were primarily distributed within a cortical layer beneath the plasma membrane, and largely ran along the long axes of dendrites, though crossing filaments were also observed (Fig. 1B, C). Our observations here were focused on dendritic shafts and do not exclude the possibility of different actin organizations in dendritic spines (3, 6).

In contrast, a drastically different organization of actin was observed in axons. Actin filaments appeared to be arranged into isolated rings that wrapped around the circumference of the axons (Fig. 1E, G). These rings were periodically distributed along the axonal shafts, forming a ladder-like, quasi-one-dimensional (quasi-1D) lattice with a long-range order (Fig. 1E, G). Examination of neurons at different developmental stages showed that the periodic actin pattern started to appear at ~5 DIV, became clearly visible at ~7 DIV (Fig. S2) (28), and was maintained in older mature neurons (e.g., 28 DIV; Fig. S3) (28). In mature neurons, more than 80% of the neuronal processes that could be identified as axon shafts (i.e. neurites positive of NrCAM, or neurites devoid of MAP2 and wider than 50 nm) exhibited the periodic, ladder-like actin pattern, whereas some filopodia-like processes branching from axon shafts did not (Fig. S3). While long actin filaments were also observed along some axons, especially in the thicker axons (Fig. 1E, G, and Figs. S2E, S3B), the periodic, ring-like pattern was the most pronounced actin feature in the axon shafts. Similar

periodic patterns were observed both in the initial segments of axons (Fig. 1G) and in distal axons that were not close to the cell body (Fig. S1B, S3).

The periodicity of the actin pattern in axons appeared highly regular (Fig. 2). Projection of the 3D images of actin to the long axis of the axon led to well separated peaks with nearly identical spacing (Fig. 2A). A Fourier transform of the 1D projection yielded fundamental frequencies and overtones that corresponded to a spatial period of ~180–190 nm (Fig. 2B). Statistical analysis of the spacings showed a narrow distribution with a mean value of 182 nm and a standard deviation of 16 nm (Fig. 2C).

The quasi-1D, periodic actin structure prompted us to search for a molecular mechanism underlying this organization. In particular, the isolated actin ring-like structures with ~180–190 nm spacing did not appear to form a cohesive network by themselves. We thus reasoned that a linker component may be present to both connect the actin structures into a network, thereby giving mechanical support to the membrane, and to provide a mechanism for the regular spacing between the actin rings. We hypothesized that spectrin could be a good candidate for this linker component. The rod-shaped spectrin tetramers, typically 150–250 nm in length, cross-link short actin filaments in the erythrocyte membrane cytoskeleton to form a 2D, polygonal network (9–12). Spectrin analogues, in particular αII-βII spectrin, are present in the mammalian brain (10, 13, 14). Moreover, brain spectrin interacts with actin, and spectrin tetramers isolated from the brain exhibit a rod-like shape, with average length 195 nm (14), comparable to the spatial periodicity we observed for the actin rings.

To test this hypothesis, we performed 3D STORM imaging of βII-spectrin, which is enriched in distal axons (31). We immunolabeled βII-spectrin using an antibody (28) that specifically targeted the C-terminus of βII-spectrin, which should label the center of the rod-like αII-βII spectrin tetramer (9, 10). If the adjacent actin rings are connected by spectrin tetramers, we expect the centers of the spectrin tetramers to also form a periodic pattern of ring-like structures with a quantitatively similar periodicity. Highly periodic, ring-like structures were indeed observed for the C-terminus of βII-spectrin in axons (Fig. 3A and Figs. S4, S5) but not in dendrites (Fig. S5) (28). Statistics of the spacings between adjacent rings gave a mean value of 182 nm and a standard deviation of 18 nm (Fig. 3B), which are nearly identical to the values measured for the actin rings (Fig. 2C), suggesting that spectrin and actin may indeed form a coordinated periodic network. βIV-spectrin, a spectrin subtype specifically located in the axon initial segment (Fig. S6) (15, 28, 32), also exhibited a quasi-1D, periodic pattern (Fig. 3C, D) similar to those of actin and βII-spectrin, consistent with the observation that the periodic actin structure was observed in both axon initial segments (Fig. 1G) and distal axons (Figs. S1B, S3).

In the erythrocyte cytoskeleton, the network formed by short actin filaments (12–16 monomers) and spectrin tetramers contains other proteins, such as adducin, a protein that caps the growing end of actin filaments and promotes the binding of spectrin to actin, and ankyrin, a protein that helps anchoring spectrin to the membrane (9, 10). We thus also probed the distributions of these molecules in axons. Immunolabeled adducin formed periodic, ladder-like structures in axons (Fig. 3E), with a periodicity quantitatively similar to those of the actin and spectrin structures (Fig. 3F). Immunolabeled ankyrin-B exhibited a semi-periodic pattern with a similar periodicity but a less regular distribution compared to those observed for actin, spectrin and adducin (Fig. S7) (28). The less regular distribution is expected for ankyrin-B because each spectrin tetramer contains two separate ankyrin-binding sites that are both away from the center of the spectrin tetramer, neither of which is necessarily occupied by ankyrin (9, 10).

To confirm that the periodic actin-spectrin structure exists in the brain, we performed STORM imaging of hippocampal tissue slices of adult mice (Fig. S8) (28). Because axons, dendrites and cell bodies are densely packed in all three dimensions in brain tissues, we needed a positive marker to unambiguously mark axons in these experiments. We used βIV-spectrin, which is specifically localized to the initial segments of axons (Fig. S6) (15, 28, 32), as such a marker. STORM imaging was performed on either immunolabeled βIV-spectrin or phalloidin-labeled actin. Indeed, quasi-1D, periodic structures were observed for both βIV-spectrin (Fig. S8A, B) and actin (Fig. S8G, I) in axon segments stained by βIV-spectrin, with periodicities quantitatively similar to those observed in cultured neurons (Fig. S8C–E, J–L).

Next, we performed two-color STORM imaging of cultured neurons to determine the relative positions of the molecular components observed in the quasi-1D, periodic axonal cytoskeleton. To this end, we labeled actin and spectrin (or adducin) with spectrally distinct photoswitchable dyes (28). Highly regular, alternating patterns of actin and spectrin were observed in axons with the spectrin stripes falling midway between adjacent actin stripes (Fig. 4A and Fig. S9A) (28). Given that the antibody specifically labeled the C-terminal region of the βII-spectrin, which is at the center of the αII-βII spectrin tetramer, and that the spacing between adjacent actin stripes was comparable to the length of the spectrin tetramer, our observations suggest that spectrin tetramers are aligned longitudinally along the axonal shaft and connect the adjacent actin ring-like structures. Treatment with an actin-depolymerizing drug, latrunculin A not only eliminated the periodic actin structures, but also disrupted the periodic structures of spectrin (Fig. S10) (28), suggesting that the actin and spectrin structures are indeed interconnected.

The adducin stripes, on the other hand, appeared to colocalize with the actin stripes (Fig. 4B and Fig. S9B) (28). Given that adducin caps one end of actin filaments, this result suggests that the ring-like actin structures likely do not represent long, continuous filaments spanning the entire ring, but are made of capped, short filaments aligned along the circumferential direction of the axon, probably facilitated by actin-binding or -crosslinking proteins (2, 3). As described earlier, long actin filaments running along axons were sometimes observed, but they did not appear to have a well-defined spatial relationship with either spectrin or adducin (Fig. S9A, B). Consistent with the above results, βII-spectrin (C-terminus) and adducin stripes also alternated with each other along the axon (Fig. 4C and Fig. S9C) (28).

To further analyze the data quantitatively, we calculated the cross-correlation between the two color channels for each of the three combinations, actin/spectrin, actin/adducin, and spectrin/adducin (Fig. 4E). The cross-correlation was determined for the 1D localization distributions as shown in Fig. S9 (28). The ~180–190 nm periodicities were apparent for all three correlation functions (Fig. 4E). The actin-adducin pair appeared correlated, exhibiting a maximum near zero shift, indicating that actin and adducin indeed colocalize with each other. The actin-spectrin (C-terminus of βII-spectrin) and adducin-spectrin (C-terminus of βII-spectrin) pairs were both anticorrelated, exhibiting a minimum at zero shift and maximum at ~90–100 nm shifts, indicating that the centers of the spectrin tetramers lie halfway between the adjacent actin-adducin rings.

Finally, to assess the possible functional implication of this quasi-1D, periodic cytoskeletal structure, we performed two-color imaging of βIV-spectrin and sodium channels (Na_v) in the axon initial segments (28). Sodium channels are enriched in the axon initial segments and are important for the generation of action potentials (15, 33). We immunostained the N-terminal region of βIV-spectrin, which is at the two ends of the spectrin tetramer. Interestingly, Na_v and the N-terminus of βIV-spectrin exhibited alternating periodic patterns with Na_v being most abundant approximately halfway between the ends of the spectrin

tetramers (Fig. 4D, E and Fig. S9D) (28). The periodic distribution of Na_V is thus most likely coordinated by the underlying periodic cytoskeleton structure, presumably through ankyrin-G (34), which interacts with both sodium channels and βIV-spectrin (9, 15, 35, 36). The periodic pattern of Na_V appeared less regular than that of βIV-spectrin, potentially because each spectrin tetramer contains two separate Na_V binding sites (through ankyrin-G) which are not fully occupied, or because not every Na_V molecule is anchored to the underlying cytoskeleton. It is also possible that the antibody against Na_V was less specific.

The above results suggest that the cortical cytoskeleton of axons is comprised of short actin filaments that are capped by adducin at one end and arranged into ring-like structures, which wrap around the circumference of the axon (Fig. 4F). Spectrin tetramers connect the neighboring actin/adducin rings along the long axis of the axon, tightly regulating the periodicity of the cytoskeleton structure to ~180–190 nm and giving the axonal cytoskeleton a long-range order. Despite the molecular composition differences between the axon initial segments and distal axons, for example ankyrin-G and βIV-spectrin are confined in the axon initial segment by an exclusion effect of the distal axon proteins ankyrin-B and βII-spectrin (31), the cytoskeletal organization is similar between the initial and distal segments of the axons, both adopting a quasi-1D, periodic structure. Interestingly, this periodic cytoskeleton structure was only observed in axons, but not in dendrites, which instead primarily contained long actin filaments running along the dendritic axis. Although the microscopic interactions between the molecular components of the axon cytoskeleton are likely similar to those between the erythrocyte analogues (9, 10), the overall structure of this quasi-1D, periodic cytoskeleton in axons is distinct from the 2D, pentagonal/hexagonal structure observed for the erythrocyte membrane cytoskeleton (11, 12). In Drosophila motoneuron axons near the neuromuscular junctions, spectrin and ankyrin appear to organize into an erythrocyte-like, pentagonal/hexagonal lattice structure (16), which is distinct from the quasi-1D, periodic, ladder-like structure that we observed in the axons of vertebrate brains. Whether the difference is due to invertebrate versus vertebrate animals or peripheral versus central nervous systems awaits future investigations.

The periodic, actin-spectrin-based cytoskeleton observed here is unlikely to be involved in myosin-dependent axonal transport. If the analogy to the erythrocyte membrane cytoskeleton holds, the capped short actin filaments in the ring-like actin structures in axons are likely bound by tropomyosin (9, 10), which may prevent the binding of myosins. Myosin-dependent axonal transport could, however, be mediated by the long actin filaments that were observed to run along the axon shaft. The quasi-one-dimensional, periodic, actin-spectrin cytoskeleton may instead provide elastic and stable mechanical support for the axon membrane, given the flexibility of spectrin. Elastic and stable support is particularly important for axons because they can be extremely long and thin, and have to withstand mechanical strains as animals move (37). Indeed, loss of β-spectrin in *C. elegans* leads to spontaneous breaking of axons, which is caused by mechanical strains generated by animal movement and can be prevented by paralyzing the animal (37). The highly periodical sub-membrane cytoskeleton can also influence the molecular organization of the plasma membrane by ordering important membrane proteins along the axon. Indeed, we found that sodium channels were distributed periodically along the axon initial segment in a coordinated manner with the underlying actin-spectrin cytoskeleton. An axonal plasma membrane with periodically varying biochemical and mechanical properties may not only influence how an action potential is generated and propagated, but might also affect how axons interact with other cells.

Supplementary Material

Refer to Web version on PubMed Central for supplementary material.

Acknowledgments

We thank Dr. Matthew Rasband for providing the βIV-spectrin and sodium channel antibodies. We thank Maria Ericsson, Bobby Kasthuri, Richard Schalek, George Hao and Colenso Speer for help in the preparation of hippocampal tissue slices. This work is supported in part by the National Institutes of Health and the Collaborative Innovation Award from Howard Hughes Medical Institute (HHMI). X.Z. is a HHMI investigator.

References

1. Pollard TD, Cooper JA. Science. 2009; 326:1208. [PubMed: 19965462]
2. Dent EW, Gertler FB. Neuron. 2003; 40:209. [PubMed: 14556705]
3. Cingolani LA, Goda Y. Nat Rev Neurosci. 2008; 9:344. [PubMed: 18425089]
4. Kapitein LC, Hoogenraad CC. Mol Cell Neurosci. 2011; 46:9. [PubMed: 20817096]
5. Lewis AK, Bridgman PC. J Cell Biol. 1992; 119:1219. [PubMed: 1447299]
6. Korobova F, Svitkina T. Mol Biol Cell. 2010; 21:165. [PubMed: 19889835]
7. Hirokawa N. J Cell Biol. 1982; 94:129. [PubMed: 6181077]
8. Schnapp BJ, Reese TS. J Cell Biol. 1982; 94:667. [PubMed: 6182148]
9. Bennett V, Baines AJ. Physiol Rev. 2001; 81:1353. [PubMed: 11427698]
10. Baines AJ. Protoplasma. 2010; 244:99. [PubMed: 20668894]
11. Byers TJ, Branton D. Proc Natl Acad Sci U S A. 1985; 82:6153. [PubMed: 3862123]
12. Liu SC, Derick LH, Palek J. J Cell Biol. 1987; 104:527. [PubMed: 2434513]
13. Levine J, Willard M. J Cell Biol. 1981; 90:631. [PubMed: 6169732]
14. Bennett V, Davis J, Fowler WE. Nature. 1982; 299:126. [PubMed: 7110333]
15. Rasband MN. Nat Rev Neurosci. 2010; 11:552. [PubMed: 20631711]
16. Pielage J, et al. Neuron. 2008; 58:195. [PubMed: 18439405]
17. Hell SW. Nat Methods. 2009; 6:24. [PubMed: 19116611]
18. Huang B, Babcock H, Zhuang X. Cell. 2010; 143:1047. [PubMed: 21168201]
19. Tatavarty V, Kim EJ, Rodionov V, Yu J. PLoS One. 2009; 4:e7724. [PubMed: 19898630]
20. Frost NA, Shroff H, Kong HH, Betzig E, Blanpied TA. Neuron. 2010; 67:86. [PubMed: 20624594]
21. Urban NT, Willig KI, Hell SW, Nagerl UV. Biophys J. 2011; 101:1277. [PubMed: 21889466]
22. Izeddin I, et al. PLoS One. 2011; 6:e15611. [PubMed: 21264214]
23. Rust MJ, Bates M, Zhuang X. Nat Methods. 2006; 3:793. [PubMed: 16896339]
24. Betzig E, et al. Science. 2006; 313:1642. [PubMed: 16902090]
25. Hess ST, Girirajan TPK, Mason MD. Biophys J. 2006; 91:4258. [PubMed: 16980368]
26. Bates M, Huang B, Dempsey GT, Zhuang X. Science. 2007; 317:1749. [PubMed: 17702910]
27. Huang B, Wang WQ, Bates M, Zhuang X. Science. 2008; 319:810. [PubMed: 18174397]
28. Supplementary materials are available on *Science* online.
29. Xu K, Babcock HP, Zhuang X. Nat Methods. 2012; 9:185. [PubMed: 22231642]
30. Egner A, et al. Biophys J. 2007; 93:3285. [PubMed: 17660318]
31. Galiano M, et al. Cell. 2012; 149:1125. [PubMed: 22632975]
32. Berghs S, et al. J Cell Biol. 2000; 151:985. [PubMed: 11086001]
33. Kole MH, Stuart GJ. Neuron. 2012; 73:235. [PubMed: 22284179]
34. Kordeli E, Lambert S, Bennett V. J Biol Chem. 1995; 270:2352. [PubMed: 7836469]
35. Zhou DX, et al. J Cell Biol. 1998; 143:1295. [PubMed: 9832557]
36. Brachet A, et al. J Cell Biol. 2010; 191:383. [PubMed: 20956383]
37. Hammarlund M, Jorgensen EM, Bastiani MJ. J Cell Biol. 2007; 176:269. [PubMed: 17261846]
38. Small JV, Rottner K, Hahne P, Anderson KI. Microsc Res Tech. 1999; 47:3. [PubMed: 10506758]
39. Koestler SA, Auinger S, Vinzenz M, Rottner K, Small JV. Nat Cell Biol. 2008; 10:306. [PubMed: 18278037]
40. Auinger S, Small JV. Methods in Cell Biology. 2008; 88:257. [PubMed: 18617038]

41. Dempsey GT, Vaughan JC, Chen KH, Bates M, Zhuang X. Nat Methods. 2011; 8:1027. [PubMed: 22056676]

42. Dani A, Huang B, Bergan J, Dulac C, Zhuang X. Neuron. 2010; 68:843. [PubMed: 21144999]

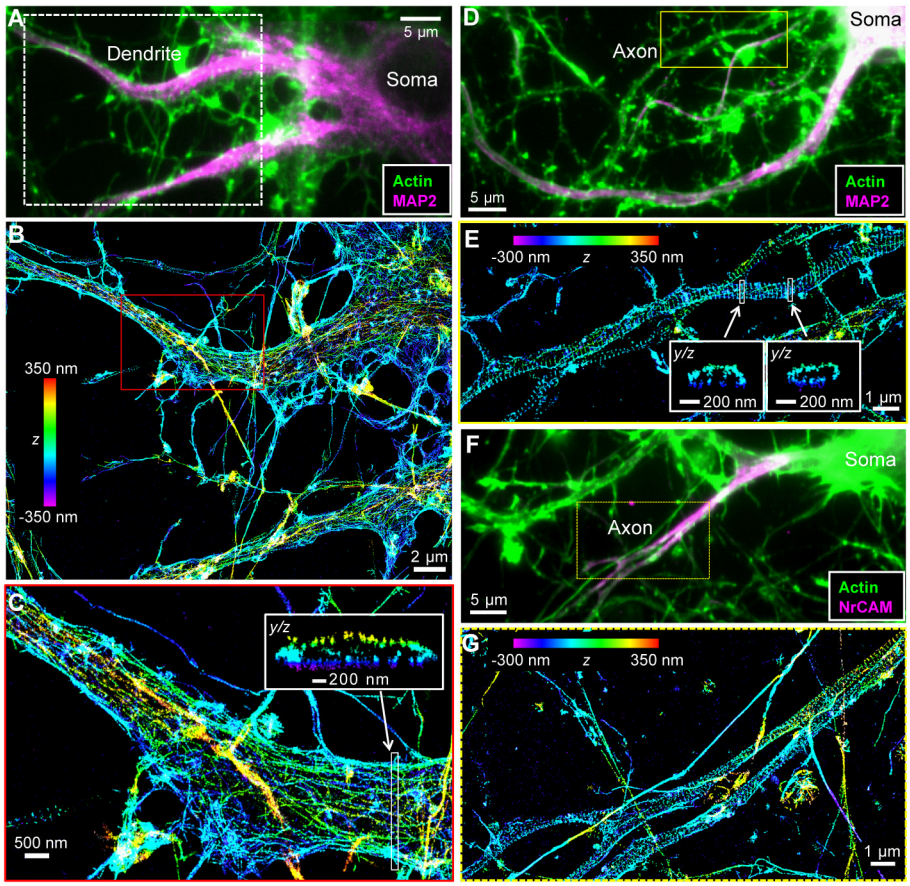

Fig. 1.

STORM imaging reveals distinct organization of actin filaments in the axons and dendrites of neurons. (**A**) Conventional fluorescence image of actin (green) and a dendritic marker, MAP2 (magenta), in a cultured hippocampal neuron fixed at 7 DIV. (**B**) 3D STORM image of actin in a dendritic region corresponding to the white box in (A). The z-positions in the STORM image are color-coded according to the color scale, with violet and red indicating positions closest to and farthest from the substratum, respectively. (**C**) Magnification of the region inside the red box in (B). The yz cross-section corresponding to the white-boxed region is shown in the inset. (**D**) Conventional fluorescence image of actin (green) and MAP2 (magenta) in a neuron fixed at 12 DIV. (**E**) 3D STORM image of actin in a region containing axons (devoid of the dendritic marker MAP2), corresponding to the yellow box in (D). The yz cross-sections corresponding to the white-boxed regions are shown in the insets. The 3D STORM image of a region containing a dendrite of this neuron is shown in Fig. S1B (28). (**F**) Conventional fluorescence image of actin (green) and an axon initial segment marker, NrCAM (magenta), in a neuron fixed at 9 DIV. (**G**) 3D STORM image of actin in a region containing the axon initial segments, corresponding to the dashed yellow box in (D).

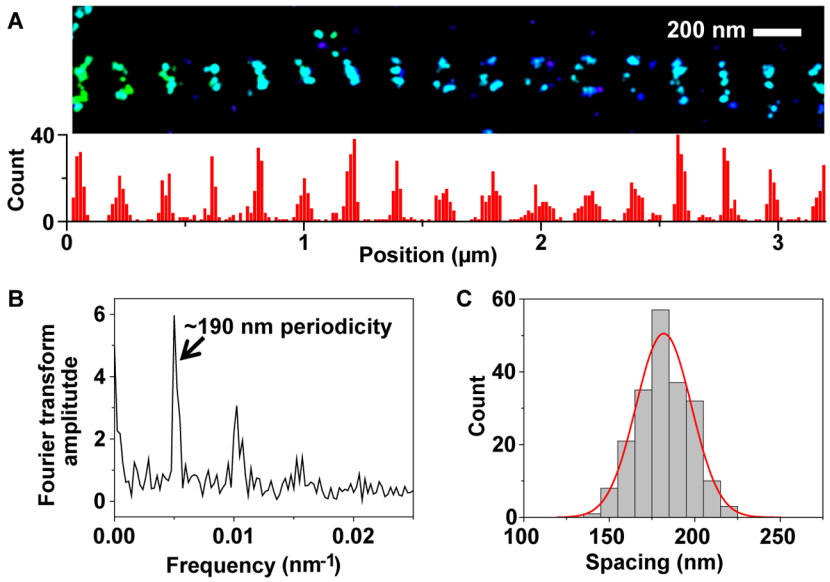

Fig. 2.

Actin filaments in axons form a quasi-1D, periodic structure with a uniform spacing of ~180–190 nm. (**A**) 3D STORM image of a segment of axon (upper panel) and the distribution of localized molecules after the 3D image was projected to one dimension along the axon long axis (lower panel). (**B**) Fourier transform of the 1D localization distribution shown in (A). The Fourier transform shows a fundamental frequency of $(190\ \text{nm})^{-1}$ and an overtone. (**C**) Histogram of the spacings between adjacent actin ring-like structures (N = 204). The red line is a Gaussian fit with mean = 182 nm and standard deviation = 16 nm.

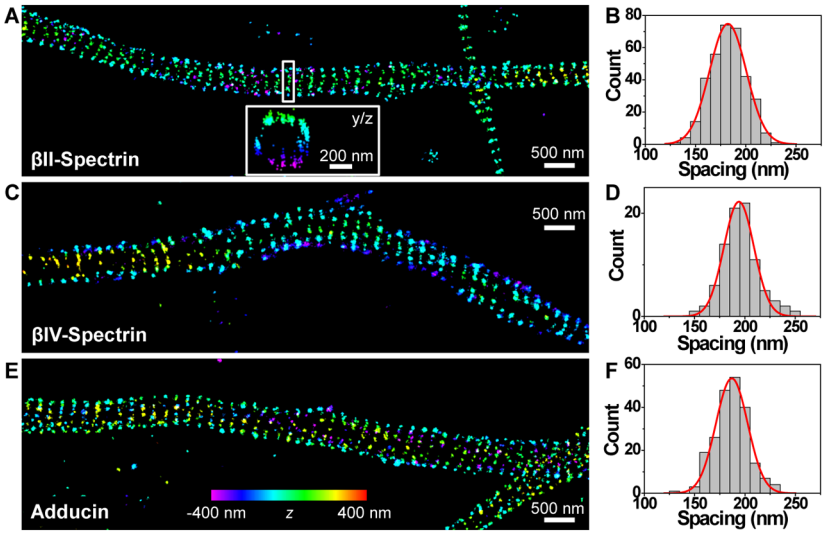

Fig. 3.

Spectrin and adducin exhibit quasi-1D, periodic patterns in axons, quantitatively similar to that observed for actin. (**A**) 3D STORM image of βII-spectrin in axons. βII-spectrin is immunostained against its C-terminal region, which is situated at the center of the rod-like αII-βII spectrin tetramer. Inset: the yz cross-section of the boxed region showing the ring-like structure. (**B**) Histogram of the spacings between adjacent spectrin rings ($N = 340$). The red line is a Gaussian fit with mean = 182 nm and standard deviation = 18 nm. (**C, D**) Same as (A, B) but for βIV-spectrin, which is specifically located in the initial segments of axons. βIV-spectrin is immunostained against its N-terminal region, which corresponds to the ends of the spectrin tetramer. The red line superimposed on the histogram is a Gaussian fit with mean = 194 nm and standard deviation = 15 nm ($N = 88$). (**E, F**) Same as (A, B) but for adducin, an actin-capping protein. The red line superimposed on the histogram is a Gaussian fit with mean = 187 nm and standard deviation = 16 nm ($N = 216$).

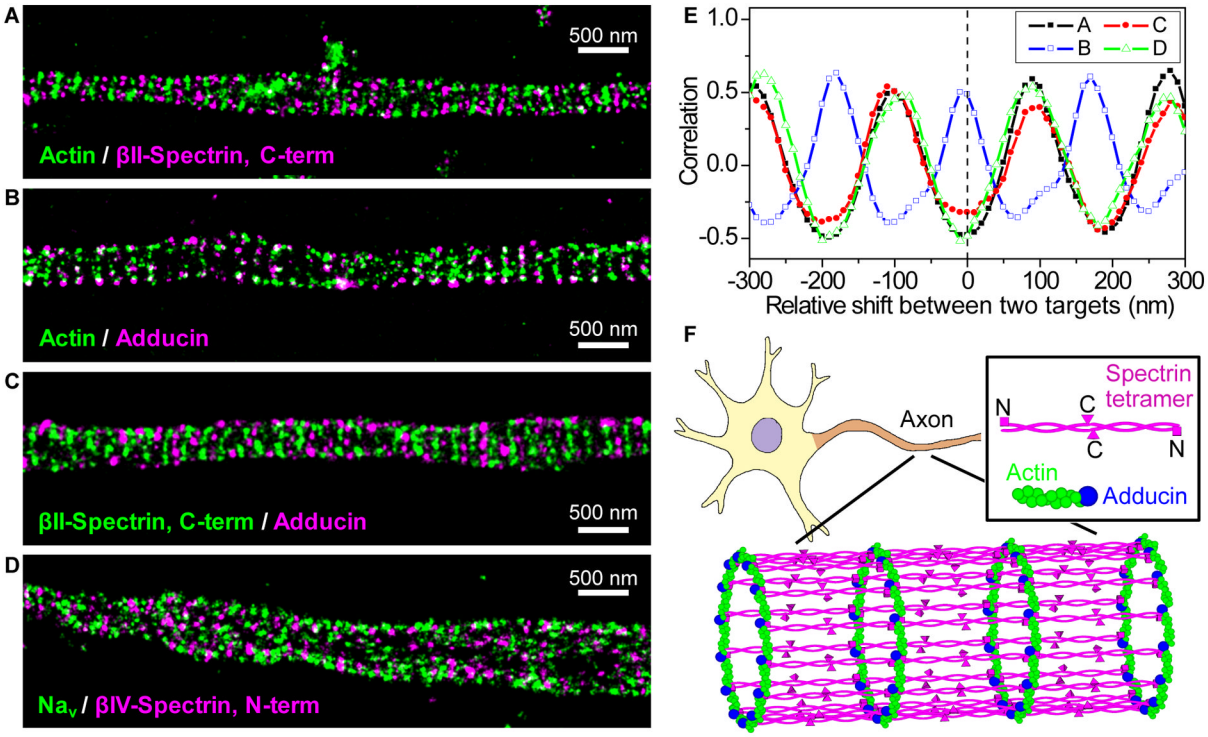

Fig. 4.

Actin, spectrin, and adducin form a coordinated, quasi-1D lattice structure in axons, and sodium channels are distributed in a periodic pattern in coordination with the actin-spectrin-based submembrane cytoskeleton. (**A**) Two-color, STORM image of actin (green) and βII-spectrin (magenta). βII-spectrin is immunostained against its C-terminal region, which is situated at the center of the spectrin tetramer. (**B**) Two-color, STORM image of actin (green) and adducin (magenta). (**C**) Two-color, STORM image of βII-spectrin (green) and adducin (magenta). (**D**) Two-color, STORM image of sodium channels (Na_v, green) and βIV-spectrin (magenta). βIV-spectrin is immunostained against its N-terminal region, which is situated at the two ends of the spectrin tetramer. The distributions of the localized molecules along the axon shafts are shown in Fig. S9 (28). (**E**) Spatial correlations between actin and βII-spectrin C-terminus (A, black), between actin and adducin (B, blue), between adducin and βII-spectrin C-terminus (C, red), and between sodium channels and βIV-spectrin N-terminus (D, green). The correlation function is calculated for varying relative shifts between the two color channels along the axons. (**F**) A model for the cortical cytoskeleton in axons. Short actin filaments (green), capped by adducin (blue) at one end, form ring-like structures wrapping around the circumference of the axon. Spectrin tetramers (magenta) connect the adjacent actin/adducin rings along the axon, creating a quasi-1D lattice structure with a periodicity of ~180–190 nm. The letters “C” and “N” in the legend mark the C-terminus (magenta triangle) and N-terminus of β-spectrin (magenta square), respectively. Ankyrin and sodium channels, not shown in the model, also form semi-periodic patterns in coordination with the periodic cytoskeletal structure.